REPORT NO. CG-D-02-89

AN EVALUATION OF THE U.S. COAST GUARD'S PHYSICAL DETECTION MODEL FOR VISUAL SEARCH

G. L. HOVER

Analysis & Technology, Inc.
190 Governor Winthrop Blvd, New London, Connecticut 06320-6223

INTERIM REPORT

MARCH 1988

Prepared for:

U.S. Department of Transportation
United States Coast Guard
Office of Engineering and Development
Washington, DC 20593

NOTICE

This document is disseminated under the sponsorship of the Department of Transportation in the interest of information exchange. The United States Government assumes no liability for its contents or use thereof.

The United States Government does not endorse products or manufacturers. Trade or manufacturers' names appear herein solely because they are considered essential to the object of this report.

The contents of this report reflect the views of the Coast Guard Research and Development Center, which is responsible for the facts and accuracy of data presented. This report does not constitute a standard, specification, or regulation.

SAMUEL F. POWEL, III
Technical Director
U.S. Coast Guard Research and Development Center
Avery Point, Groton, Connecticut 06340-6096

Technical Report Documentation Page

1. Report No.	2. Government Accession No.	3. Recipient's Catalog No.
CG-D-02-89		

4. Title and Subtitle	5. Report Date
An Evaluation of the U.S. Coast Guard's Physical Detection Model for Visual Search	March 1988
	6. Performing Organization Code
7. Author(s)	8. Performing Organization Report No.
Hover, G. L.	CGR&DC 10/88
9. Performing Organization Name and Address	10. Work Unit No. (TRAIS)
U.S.C.G. R&D Center, Avery Point, Groton, CT 06340-6096 / Analysis & Technology, Inc., 190 Governor Winthrop Blvd., New London, CT 06320-6223	11. Contract or Grant No. DTCG39-83-C-80863
12. Sponsoring Agency Name and Address	13. Type of Report and Period Covered
Department of Transportation, U.S. Coast Guard, Office of Engineering and Development, Washington, D.C. 20593	Interim Report, Sept. 1987 - March 1988
	14. Sponsoring Agency Code

15. Supplementary Notes

This report is the twenty-fourth in a series which documents the Improvement in Probability of Detection in Search and Rescue (POD/SAR) Project at the U.S.C.G. R&D Center.

16. Abstract

In 1983, an analytical method for modeling visual search/detection performance was developed for the U.S Coast Guard. This method, known as the physical detection model, was implemented in a computer software package called VSW. VSW is resident on the Coast Guard's PRIME computer facility at Governor's Island, N.Y.

This study analyzes the foundations of the physical detection model, its mathematical modeling approach, and its computational methods. Software corrections and modifications made in conjunction with this study are documented and discussed. A comparison of sweep widths and lateral range curves predicted by the model to those actually achieved during two recent visual detection experiments is provided.

Recommendations for improving model accuracy and applicability are made.

17. Key Words	18. Distribution Statement
Search and Rescue, Visual Detection, Sweep Width, Visual Search, Detection Modeling	Document is available to the U.S. Public through the National Technical Information Service, Springfield, VA 22161

19. Security Classif. (of this report)	20. Security Classif. (of this page)	21. No. of Pages	22. Price
UNCLASSIFIED	UNCLASSIFIED		

Form DOT F 1700.7 (8-72) Reproduction of form and completed page is authorized

322 532

METRIC CONVERSION FACTORS

Approximate Conversions to Metric Measures

Symbol	When You Know	Multiply By	To Find	Symbol
	LENGTH			
in	inches	*2.5	centimeters	cm
ft	feet	30	centimeters	cm
yd	yards	0.9	meters	m
mi	miles	1.6	kilometers	km
	AREA			
in^2	square inches	6.5	square centimeters	cm^2
ft^2	square feet	0.09	square meters	m^2
yd^2	square yards	0.8	square meters	m^2
mi^2	square miles	2.6	square kilometers	km^2
	acres	0.4	hectares	ha
	MASS (WEIGHT)			
oz	ounces	28	grams	g
lb	pounds	0.45	kilograms	kg
	short tons (2000 lb)	0.9	tonnes	t
	VOLUME			
tsp	teaspoons	5	milliliters	ml
tbsp	tablespoons	15	milliliters	ml
fl oz	fluid ounces	30	milliliters	ml
c	cups	0.24	liters	l
pt	pints	0.47	liters	l
qt	quarts	0.95	liters	l
gal	gallons	3.8	liters	l
ft^3	cubic feet	0.03	cubic meters	m^3
yd^3	cubic yards	0.76	cubic meters	m^3
	TEMPERATURE (EXACT)			
°F	Fahrenheit temperature	5/9 (after subtracting 32)	Celsius temperature	°C

*1 in = 2.54 (exactly). For other exact conversions and more detailed tables, see NBS Misc. Publ. 286, Units of Weights and Measures. Price $2.25. SD Catalog No. C13.10:286

Approximate Conversions from Metric Measures

Symbol	When You Know	Multiply By	To Find	Symbol
	LENGTH			
mm	millimeters	0.04	inches	in
cm	centimeters	0.4	inches	in
m	meters	3.3	feet	ft
m	meters	1.1	yards	yd
km	kilometers	0.6	miles	mi
	AREA			
cm^2	square centimeters	0.16	square inches	in^2
m^2	square meters	1.2	square yards	yd^2
km^2	square kilometers	0.4	square miles	mi^2
ha	hectares (10,000 m^2)	2.5	acres	
	MASS (WEIGHT)			
g	grams	0.035	ounces	oz
kg	kilograms	2.2	pounds	lb
t	tonnes (1000 kg)	1.1	short tons	
	VOLUME			
ml	milliliters	0.03	fluid ounces	fl oz
l	liters	0.125	cups	c
l	liters	2.1	pints	pt
l	liters	1.06	quarts	qt
l	liters	0.26	gallons	gal
m^3	cubic meters	35	cubic feet	ft^3
m^3	cubic meters	1.3	cubic yards	yd^3
	TEMPERATURE (EXACT)			
°C	Celsius temperature	9/5 (then add 32)	Fahrenheit temperature	°F

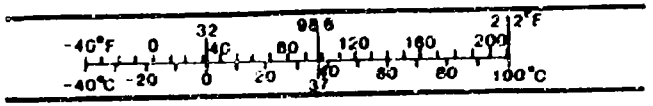

TABLE OF CONTENTS

LIST OF ILLUSTRATIONS

LIST OF TABLES

ACKNOWLEDGEMENTS

The author would like to acknowledge the valuable gu ance provided by the technical sponsor of this work, Mr. R. Q. Robe of the USCG Research and Development Center. Thanks is also due to the Commander, International Ice Patrol (IIP) for providing access to the Coast Guard computer facility at Governor's Island, NY, through the IIP's C-3 terminals. In particular, the expert gui·'nce on the use of the C-3 terminal provided by MSTCS G. Wright is gratefully acknowledged. Finally, thanks is due to Mssrs. R. Muscarella, H. Searle, and R. Volk of Analysis & Technology, Inc., for their technical support and review roles in this research.

CHAPTER 1
INTRODUCTION

1.1 SCOPE AND OBJECTIVES

This report provides an analysis and evaluation of the analytical visual detection model currently used by the U.S. Coast Guard to compute sweep width for overwater search problems that have not been specifically evaluated during field experiments. This visual detection model, documented in reference 1, is known as the "physical detection model" because it attempts to mathematically model the physical process by which the human eye perceives a target.

During model development, outputs were adjusted using visual search data collected by the U.S. Coast Guard Research and Development Center (R&D Center) between 1978 and 1981. Since that time, additional visual detection experiments have been conducted by the R&D Center and the Canadian Coast Guard (references 2 and 3) that provide an opportunity to evaluate the physical detection model's accuracy in extrapolating sweep width estimates to untested targets and environmental conditions.

The two objectives of this report are:

1. To provide an independent analysis of the modeling software and the modeling method used, identifying model limitations and risks, and

2. To evaluate the model's ability to extrapolate sweep width to untested search situations by comparing model predictions to actual field test results.

1.2 PHYSICAL DETECTION MODEL DESCRIPTION

The Coast Guard's physical detection model is based on laboratory research and mathematical modeling described by Koopman in his widely-read OEG Report 56 (reference 4), published in 1946. In reference 1, Weisinger describes in detail how Koopman's detection lobe model was adapted to provide overwater sweep width estimates for Coast Guard applications. This adaptation of the detection lobe model for Coast Guard use was performed by D.H. Wagner Associates in 1983. The model was "calibrated" using visual search data collected by the R&D Center during six field experiments conducted from 1978 to 1981 (references 5 through 8).

The physical detection model uses an expression derived in reference 4 to compute the probability that a moving searcher (who is looking continuously) will detect a target. This expression is:

$$P = 1 - \exp\left[-k \int_{t_1}^{t_2} f(t)dt\right] \quad (1)$$

where

k = a constant that must be estimated from available search data incorporating the effects of sea state, search platform characteristics, human factors, and other factors influencing the detection process;

t_1, t_2 = start and end times of a searcher-target encounter, i.e., a "sweep" by the searcher past the target; and

$f(t)$ = a time-varying function of physical search parameters including meteorological visibility, target area, searcher altitude, target range, and intrinsic contrast of the target.

The value of P is computed for a sweep past the target at a specified lateral range r. Lateral range is defined as the distance between searcher and target at the closest point of approach during a sweep (see figure 1-1). When P(r) is computed for all meaningful values of r, a probability of detection versus lateral range curve is defined (see figure 1-2). Sweep width for a particular search situation is defined as

$$W = \int_0^{r_{max}} P(r)dr \quad (2)$$

where

W = sweep width, a measure of search capability;

$P(r)$ = probability of detecting a target during a sweep made at lateral range r; and

r_{max} = the practical limit of meaningful lateral range values. This value might be the meteorological visibility limit, the horizon distance determined by searcher altitude and the earth's curvature, or some other physical limit to the range at which the target can be seen. Its value depends on searcher characteristics, target characteristics, and environmental conditions.

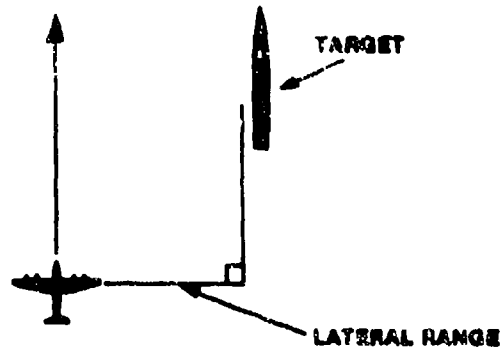

Figure 1-1. Definition of Lateral Range

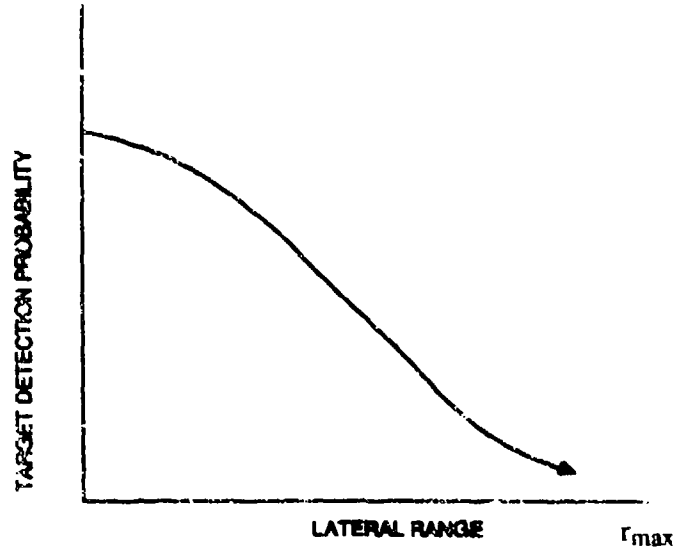

Figure 1-2. Example of a Lateral Range Curve For Visual Detection

The factor of 2 in front of the integral reflects a detection capability to both sides of a searcher's path. The concepts of lateral range curves and sweep width are described in detail in reference 4.

The detection lobe modeling methodology focuses on the f(t) term in equation 1. The model defines this function as

$$f(t) = \theta\,[R(t)] \tag{3}$$

where $\theta[R(t)]$ is a measure of the angular size of the eye's detection lobe at a specific time t. Figure 1-3, taken from reference 1, illustrates this concept. Under daylight conditions, the eye can detect objects within a wide angular field when they are at relatively close range. As range to the target increases, the angular size of the eye's detection lobe diminishes.

The model's equation for $\theta[R(t)]$ is a combination of simple geometric considerations with a somewhat cumbersome expression that was empirically derived from World War II-era laboratory research on visual detection. The value of $\theta[R(t)]$ is restricted to a range of 0 to 90 degrees and depends on the following search problem variables:

V = meteorological visibility (nmi),

A_H = horizontal plane area of target (sq. ft.),

A_V = vertical plane area of target (sq. ft.),

h = searcher height (ft.),

$R(t)$ = slant range to target at time t (nmi), and

C_C = intrinsic contrast between target and background.

The variables listed above are the only search problem parameters that are explicitly considered in the detection lobe model. The constant term k in equation 1 must incorporate, in an indirect fashion, the effects of sea state, search platform characteristics, human factors, and any other remaining parameters that influence the visual search/detection process. It should also be noted that the detection lobe model assumes continuous looking by a single searcher.

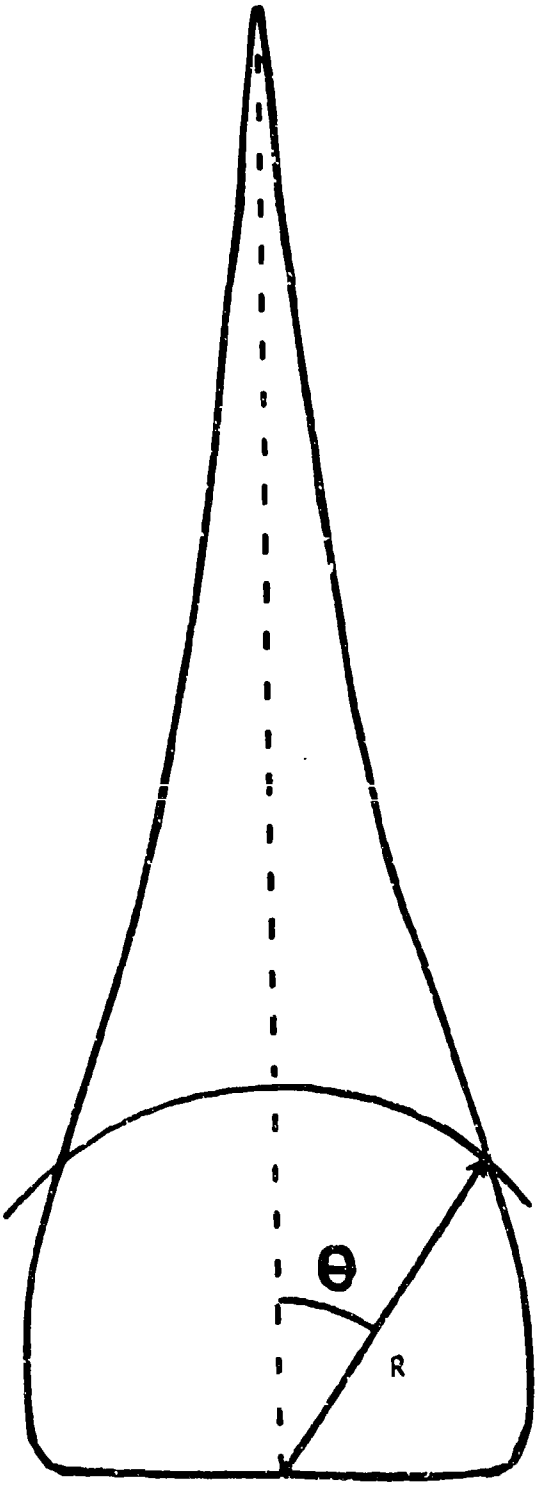

Figure 1-3. Example of a Visual Detection Lobe (from reference 1)

An analysis of the physical detection model and its assumptions, limitations, and risks is provided in chapter 2.

1.3 VSW SOFTWARE DESCRIPTION

The physical detection model was integrated by D.H. Wagner Associates into a software package called VSW. The VSW software performs two main tasks:

1. Computing values of k using visual search data collected during field experiments, and

2. Computing sweep width for user-specified sets of search parameter values.

Figure 1-4 provides a high-level processing flow diagram for the VSW software package. The user selects the desired option (1 or 2) and provides required inputs interactively through the computer terminal. Option 1 of the program outputs a value of k and (optionally) the lower and upper 95-percent confidence bounds on k for the search data set selected. Option 2 of the program outputs a sweep width value and (optionally) the lower and upper 95-percent confidence bounds on W for the user-specified search parameter values. If confidence bounds on W are desired, they must first be computed for k in option 1. Each option returns the user to the main program (point "A" in figure 1-4) until the QUIT option is selected.

Reference 9 provides detailed user instructions for the VSW software package. Software documentation is provided by means of extensive comments statements within the FORTRAN-77 source code (reference 10). The program presently resides in the PRIME computer facility at U.S. Coast Guard LANTAREA Operations Computer Center (OCC), Governors Island, NY.

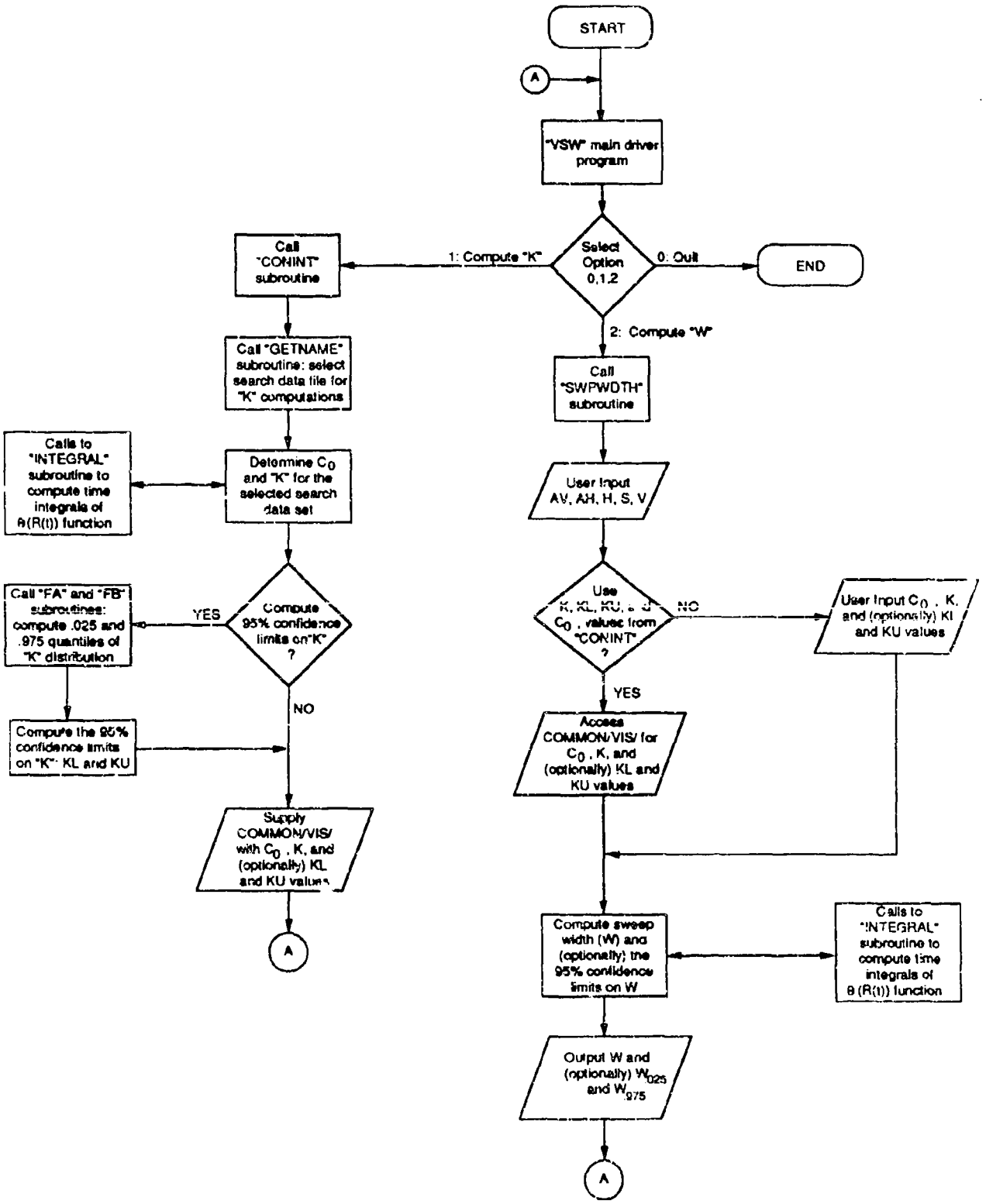

Figure 1-4. VSW Software Flow Diagram

[BLANK]

CHAPTER 2
ANALYSIS OF THE PHYSICAL DETECTION MODEL

2.1 MODEL FOUNDATIONS

The detection lobe model described in section 1.2 was developed by Koopman in 1946 using laboratory data obtained from experiments conducted by K.J.W. Craik and others during World War II. These experiments were designed to measure the threshold contrast required to detect a target of specified angular size. From these data, Koopman developed equations that related target intrinsic contrast (C_0), target range (R), meteorological visibility (V), and target apparent area (A) to the visual perception angle θ. The angle θ is measured in degrees from the center of the fovea (a portion of the eye's retina that provides the finest spatial resolution for vision) to the center of the target image. The value of θ represents the angular half-width (in degrees) of the visual detection lobe depicted in figure 1-3 for a given combination of the parameters listed above.

The expression for $\theta[R(t)]$ provided in reference 1 is developed from Koopman's work as reported in chapter 4 of reference 4. This expression is:

$$\theta(R) = \begin{cases} 0 \text{ if } \beta^2(R) < 0.8 \\ \beta^2(R) \text{ if } 0.8 \le \beta^2(R) \le 90 \\ 90 \text{ if } \beta^2(R) > 90 \end{cases} \tag{4}$$

where

$$\beta(R) = \left[-1.75\,\alpha^2 + \alpha(3.0625\alpha^2 + 76C_0 e^{-3.44R/V})^{1/2}\right] / 38\,, \tag{5}$$

$$\alpha(R) = 0.64\sqrt{A}/R\,, \tag{6}$$

and

$$A = A_H\, h/R + A_V\left[1 - (h/R)^2\right]^{1/2}. \tag{7}$$

The time-dependent variable in these expressions is the target range R, hence the term $\theta[R(t)]$ in equation 3. Equation 6 for the visual angle α approximates the angle (in minutes) subtended by a circular target of area A (in sq. ft.) at range R (in nmi). Equation 7 is an expression for the apparent area A of the target when viewed from altitude h (in ft.) at range R.

Equation 5 arises from Craik's empirical expression relating θ, α, and the target threshold contrast required for detection. This expression is:

$$C = 1.75\ \theta^{1/2} + 19\theta/\alpha^2 \ . \qquad (8)$$

If one substitutes the variable β for $\theta^{1/2}$ and incorporates the empirical relation $C = C_0 e^{-3.44R/V}$, the quadratic formula yields equation 5 when β is solved for. Squaring β yields the desired value of θ as shown in equation 4.

As Koopman states in reference 4, "...(Craik's expression) is purely empirical. ... Since the number of measurements made by Craik is relatively small, the experimental error is fairly high: Hence slight modifications...are to be expected... ." To the best of this author's knowledge, such modifications, if any were ever made, have not been incorporated into the physical detection model. In appendix E of his 1980 book, Search and Screening (reference 11), Koopman cites a good deal of contrast threshold research that was conducted after 1946, but does not re-work the detection lobe model to reflect the new research. The updated work indicates only that the 3.44 factor in the exponential term of equation 5 has changed to 3.912. In fact, it is worth noting that in reference 11 Koopman states "...because of the multiplicity of variables that affect visual target detection, even without the added complication of the search situation, it is not always possible to extrapolate from laboratory data to actual field conditions to obtain predictions of detection performance with useful precision." In 1981, Koopman proposed an alternate empirical method for obtaining f(t) for equation 1. This method was considered in reference 1 but was rejected in favor of the detection lobe model based on a comparison of both models with the R&D Center field experiment data.

Another aspect of the physical detection model to remember is its assumption concerning the searcher's scan pattern. In the model, the $\theta[R(t)]$ function is integrated continuously over the duration of a searcher-target encounter: this amounts to an assumption of a single searcher who is always looking in the direction of the target. Research conducted by the U.S. Army Aeromedical Research Laboratory (USAARL) in cooperation with the R&D Center (reference 12) demonstrated that this continuous looking assumption is not realistic. Also, the assumption is not consistent

with proper scanning techniques. The only available means of adjusting physical detection model outputs for the effects of searcher scan techniques and variable numbers of lookouts is through the constant term k, which must be computed from field experiment data. Koopman acknowledges this in section 4.9 of reference 4.

2.2 CRITICAL INPUT PARAMETERS

As discussed in section 1.2, the physical detection model uses a number of input variables to compute the value of W. These variables can be classified as search problem parameters that are explicitly considered in the model and one (k) that must account for all aspects of the search/detection process that are not explicitly modeled. The following paragraphs discuss the accuracy with which each of these model inputs can be determined for a given search problem.

Meteorological Visibility (V). In reference 11, Koopman provides a practical definition of V as the range at which a large, distant, black object is just recognizable against the horizon sky. This quantity can usually be estimated reasonably well for a given search problem.

Target Area (A_H, A_V). The horizontal and vertical plane areas of the target can be determined with very good accuracy when the target is known.

Searcher Height (h). This parameter is a known search platform characteristic for surface searchers and a selectable parameter for aircraft. Its value is known very accurately in either case.

Slant Range at Time t (R(t)). This quantity depends on the searcher's speed (S), the lateral range, and the value of h for a particular sweep past the target. Since these three quantities can be accurately determined, R(t) can be computed with good accuracy.

Intrinsic Contrast of the Target (C_0). This quantity must be measured in the field to obtain accurate values. In reference 4, Koopman addresses the case of surface targets that are underway. In this case, the wake rather than the vessel itself becomes the dominant target. Koopman defines intrinsic contrast as:

$$C_0 = \frac{B_{object} - B_{background}}{B_{sky}}$$

where B denotes brightness. Citing field measurements, Koopman notes that for look angles from the horizon to 45 degrees below the horizon, the sea background is about 0.5 times that of the sky. Further, he states that a wake reflects nearly all incident light, therefore B_{object} equals B_{sky} for a wake target. Substituting these values into the above equation, Koopman gets

$$C_0 \text{ (wake)} = \frac{1 - 0.5}{1} = 0.5 \text{ or } 50 \text{ percent}.$$

In reference 1, Weisinger assigns C_0 values of 20 percent to person-in-water (PIW) targets and 40 percent to boats and life rafts. No explanation of how these values were determined is given, other than stating that "An analysis of Coast Guard visual detection data suggests that $C_0 = 20$ for persons in the water and $C_0 = 40$ for boats and rafts are reasonable values." In reality, C_0 can be expected to vary considerably during a searcher-target encounter, especially when short ranges and look angles of more than 45 degrees below the horizon come into play. For example, in reference 4 Koopman states that field measurements of sea brightness decreased from 50 percent to 4 percent of the sky brightness as look angle varied from 45 degrees below the horizon to directly underneath the observer. This variation, in turn, will affect the value of C_0 for a given target, as range decreases. Color contrast between target and background is not considered at all in the physical detection model. Color contrast will be addressed in section 2.3. C_0 values currently used in the physical detection model are, at best, educated guesses with no specific field measurement data to support them.

Constant Term (k). As stated earlier, k must account for all search problem variables other than those listed above. The only means of determining k for a specific combination of search platform type, target type, environmental conditions, and human factors considerations is to collect a set of visual search data in the field. Thus, as reference 1 acknowledges, the ability of the physical detection model to extrapolate W-values to untested search problems is confined to changes only in those parameters that are specifically considered in the model. The implicit assumption made in using the model for sweep width extrapolation is that changes in meteorological visibility, target size, search speed, search altitude, and C_0 will not significantly impact the value of k. This issue will be expanded

upon in section 2.3. Reference 1 provides the following expression for estimating k from a set of search data:

$$k = M / \sum_{i=0}^{N} \int_{s_i}^{t_i} \theta\,[R(t)]\,dt$$

where

N = total number of searcher-target encounters in the data set,

M = number of targets detected, and

s_i, t_i = start and end times of each encounter.

Recalling that equation 1 gives the probability of detecting a target as a function of the same integral of $f(t) = \theta[R(t)]$, we see that k ensures that the physical detection model will yield the correct average probability when all searcher-target encounters in the parent search data set are considered. Departures from the parent data set (as is the case when extrapolating) will diminish the accuracy of k.

2.3 MODEL LIMITATIONS AND RISKS

Sections 2.3.1 and 2.3.2 identify and discuss aspects of the existing physical detection model that can be classified as model limitations and risks. Model limitations are defined as those aspects of the visual search and detection process that are not adequately addressed in the existing model, but could be incorporated with additional literature research and/or analytical effort. Risks are defined as those characteristics of the existing physical detection model that jeopardize its ability to model the operational visual search process and predict visual sweep widths with acceptable accuracy. Limitation and risk issues are presented in order of their expected impact on model accuracy, although several may be equal in importance.

2.3.1 Model Limitations

1. **Assumptions of Continuous Looking by a Single Searcher.** As stated in section 2.1, the physical detection model does not account for movement of the searcher's detection lobe over the search area (scanning) or for periods of time when no search is taking place due to inattention, distraction, or rest. This is a complex human behavior modeling problem that would have to be researched in the literature and probably in the field. A related issue is one of weighting the equation for $\theta[R(t)]$ to reflect the number of lookouts onboard a particular type of search craft, and the possible inclusion of another weighting factor to reflect the training, experience, and visual acuity of the lookouts. Thorough investigation of these issues would constitute a major research effort.

2. **Adjustment of Effective Target Area for Earth Curvature.** The physical detection model does not presently adjust A for earth curvature to reflect its variation with searcher height, target height, and range. This is a simple physical process that can be modeled analytically.

3. **Consideration of Color Contrast.** The physical detection model presently considers only the brightness contrast between target and background. In reference 4, Koopman dismisses the importance of color contrast in the visual detection process, stating "It has long been believed that in comparison with brightness contrast, color is of little importance in determining whether or not a given target can be seen. Recent investigations have supported this belief and have shown that any effects due to color can be ignored in most operational problems of visual search without thereby introducing any appreciable errors." The basis of this statement is World War II-vintage research. The types and sizes of targets used in this research and the distances involved are unknown; they may not be representative of encounters at ranges of a few miles or less with small boats, life rafts, and persons in the water. The legitimacy of excluding color contrast from the physical detection model could be investigated through literature research. More recent studies of daytime aids to navigation might prove to be an excellent source of information.

4. **Integration Limits.** When computing target detection probability, the physical detection model gives equal weight to the portions of the searcher's track before and after closest point of approach to the target. This seldom reflects the operational situation. According to reference 7, most lookouts onboard Coast Guard search craft

concentrate their scans within the forward 210 degrees of relative bearing (255- to 105-degrees relative). Analysis of available visual search data could provide guidance concerning how various portions of the searcher's track relative to the target should be weighted when computing detection probability.

5. **Calculation of Visual Angle α.** The expression for angle α currently used in the physical detection model is merely an approximation. The exact expression for the visual angle in terms of A and R is:

$$\alpha = 120 \arctan (\sqrt{A} / 10770 R) \qquad (9)$$

where α is expressed in minutes, A in square feet, and R in nautical miles. Equation 8, which is taken directly from reference 4, results from making an approximation that the tangent of a small angle is roughly equal to the angle expressed in radians. While only small errors are likely to result from using this approximation, there is no reason not to use the exact expression given in equation 9 now that electronic calculators and computers are readily available.

2.3.2 Risks

1. **Assumptions Concerning k.** The extrapolation methodology described in chapter 1 of reference 1 suggests that once the value of k is determined for a particular combination searcher type, target type, and overall weather conditions, the physical detection model can be used to predict sweep width for untested values of V, A_H, A_V, S, h, and/or C_0. This method applies as long as the value of parameter k remains unchanged. There are two types of risk associated with the approach.

First, the methodology assumes that the value of k is completely independent of the specifically-modeled search variables. To illustrate this type of risk, consider the following example.

EXAMPLE 1. The values of k provided in reference 1 were computed from a visual search data set that included only 16-foot boat, life raft, and PIW targets. To obtain sweep width estimates for a 45-foot cabin cruiser target using the physical detection model's extrapolation methodology, we would proceed as follows.

a. Select a value of k that represents the searcher type, target type, environmental conditions, and human factors conditions we are interested in. Target type is chosen as "boat."

b Alter the values of A_V and A_H to represent the size of the 45-foot cruiser. Although we are free to change the values of V, S, h, and C_0, we will assume that they remain unchanged in this example.

c. Compute the new sweep width by running the VSW computer program with the selected parameter values.

Let us assume that this procedure was used to compute sweep width for the 45-foot target in 3-foot seas. This sea condition is well-represented in the search data sets used to compute k-values in reference 1. Now consider the impact that 3-foot seas have on the effective target area A. In the case of a 16-foot boat (the target for which our k-value was computed), we would have a target that was intermittently masked almost completely by the ocean waves. In the case of the 45-foot cabin cruiser, we would experience relatively minor fluctuations in the effective target area A. This example serves to illustrate that search problem parameters such as sea state that are incorporated into the constant k can, in fact, exert a strong influence on the behavior of specifically-modeled parameters such as A. In this particular example, one might reasonably expect the model to predict an overly-conservative value of W for the 45-foot target.

The second type of risk involves situations where the model user is unaware that the selected value of k is inappropriate for the search problem of interest. The following example illustrates this situation.

EXAMPLE 2. In 1983, the R&D Center evaluated the visual search capabilities of the recently-acquired HU-25A medium-range surveillance aircraft. Data analysis from this experiment (reference 13) was not completed in time for inclusion in the physical detection model development process. Environmental conditions and target types were essentially the same during the 1983 experiment as they were during earlier experiments that served as the basis for developing k-values for fixed-wing aircraft searches. One might reasonably expect, then, that the physical detection model could have been used to predict visual sweep widths for the HU-25A by using the appropriate k-values for fixed-wing aircraft searches. In fact, the

HU-25A achieved significantly larger sweep widths than the older HC-130 and HU-16 aircraft. This improvement was achieved in spite of using slightly higher search speeds with the new jet. At the higher search speed, the physical detection model would have predicted somewhat smaller values of W for the HU-25A because no new value of k would have been available before the experiment. In this case, the risk demonstrated is that of failure to identify a situation where new values of k are required. The specific reasons for achieving improved sweep width with the HU-25A were not determined, but were believed to be related to human factors such as improved crew comfort (due to reduced noise levels, better seating, etc.) and reduced aircraft operation workload (due to automated navigation and flight controls, etc.). There is no reliable way for a physical detection model user to predict when a new value of k is required. Only field experiments can identify this requirement and provide data for the computation of valid k-values.

2. **Accuracy of C_0 Values.** The estimates of C_0 presently used in the physical detection model appear to have no foundation in field measurements of target and background brightness. Also, as discussed in section 2.2, the physical detection model does not provide for variations in C_0 as look angle below the horizon changes during a searcher-target encounter. If one considers the case of a small target viewed from an aircraft, or any target when visibility is poor, it is likely that the only significant contributions to target detection probability will occur during the time when the target is well below the horizon. Thus, if detection probability (and the resultant sweep width) is to be computed accurately for such situations, the model must be modified to include variations in C_0 with look angle.

3. **Basis for $\theta[R(t)]$ Function.** As described in section 2.1, the empirical expression in equations 4 and 5 was developed entirely from laboratory test data under controlled conditions. The laboratory experiments measured the threshold contrast required to achieve a 57-percent detection probability when the subject knew where to look and when the target was present. These conditions are certainly not representative of the typical SAR mission, and use of such laboratory results to represent operational capability clearly involves risk. In reference 11, Koopman acknowledges the difficulty of modeling the complex process of visual search and detection: "It is apparent that although much work in visual detection has been done...much more data, particularly on field variables, and a better understanding of variables, such as alerting, training,

and search strategy, are required before very accurate estimates can be made of target detectability under field search conditions." Note that this comment was written in 1980, after Koopman had spent a career developing search theory and detection models. The equation for $\theta[R(t)]$ was developed in 1946.

4. **Model Validation Methods.** In reference 14, three test methods and four analysis methods are proposed by Wagner Associates for use in validating the physical detection model. The three test methods are:

   a. Duplicate one or more of the visual detection experiments that were used to develop the initial k-values provided in reference 1. This requires collecting visual search data with the same search platform types, environmental conditions, and target types that were used in the original R&D Center experiments. One would expect consistency in the lateral range curves and sweep widths produced by the model using the old and new experiment data sets.

   b. Conduct a visual detection experiment that differs from the original R&D Center field work only in the values of parameters explicitly considered in the physical detection model. Here we would be free to change only meteorological visibility, searcher speed and/or altitude, target size, and target intrinsic contrast. One would expect the model to accurately predict lateral range curves and sweep widths for this type of experiment.

   c. Conduct a visual detection experiment that differs from the original R&D Center field work in the values of parameters not explicitly considered in the physical detection model. Here we might select a different search platform type, change search unit manning, operate in more adverse environmental conditions, or use an unusual target shape. Since there would be no way to adjust k-values before such an experiment, one might expect the model's extrapolation accuracy to suffer in this situation.

Options **a**, **b**, and **c** represent increasing levels of risk in their likelihood of supporting the physical detection model's accuracy. Option **b** is of the greatest interest in that it supports validation of the model's advertised extrapolation capabilities. Option **a** represents only a check of previous work; while option **c** may demand more of the model than it is capable of

delivering. It should be noted, however, that the extrapolation capabilities demanded by option c represent a very real Coast Guard search planning requirement.

The four analysis methods proposed in reference 14 are described qualitatively below.

a. Detection Probability Test. Compare the proportion of detections predicted by the model for a search data set to the actual proportion of detections achieved. The test is passed (see below) if the difference between these proportions is less than two standard deviations from the expected difference of zero. The difference statistic can be assumed to be normally distributed.

b. Distribution Test. Consider only those targets in the data set that were detected by the searcher. Compare the model's predicted distribution of detection times to the actual distribution of detection times. Find the maximum value of the difference between the two distributions. If this maximum difference value does not exceed the critical value for the desired confidence level of the test, the test is passed.

c. Comparison of k Estimates. Assume that two equivalent visual detection experiments have been conducted (test method **a** described earlier). The computer program VSW is used to determine k-values for the two experiments (call these k_1 and k_2). Determine whether the quantity $k_1 - k_2$ falls between the 95-percent confidence limits for this difference plotted as a function of the true value of k. The test is passed if the difference $k_1 - k_2$ falls within its 95-percent confidence limits over the locus of true k-values expected for the experiments that were conducted. This locus of true k-values, in turn, is defined as the intersection of the 95-percent confidence limits computed for k_1 and k_2 by the VSW program.

d. Comparison of Lateral Range Curves and Sweep Widths. The most subjective but comprehensive method of analyzing model validity that is recommended in reference 14 is to simply compare the lateral range curves and sweep widths predicted by the model for a particular data set to those determined by empirical analysis of the data.

Three of the four analysis methods described above (methods **a**, **b**, and **c**) can be classified as non-parametric hypothesis tests. This methodology consists of forming a null hypothesis, H_0, stating that there is no difference between two values of some quantity of interest. In this case, the null hypotheses are that the proportion of detections, the distribution of detection times, or the value of k predicted by the model is not statistically different from the corresponding value for the actual search data set. If we cannot show, with 95-percent confidence, that H_0 is invalid, we accept H_0. Only if we can show that there is less than a 5-percent chance of H_0 being correct do we reject H_0. This "innocent until proven guilty" approach to model validation incurs a high risk of committing what is known as a Type II error; that H_0 will be accepted when in fact it is invalid.

Analysis method **d** is not completely quantitative, but is a quicker means of evaluating the physical detection model's fidelity with actual search results. By comparing modeled versus empirical lateral range curve shapes and sweep widths, one can easily determine whether the fidelity is good enough to accept outright, poor enough to reject outright, or requires more rigorous evaluation. Method **d** will be used in chapter 4 to compare model predictions to some recent field experiment results.

CHAPTER 3
MODIFICATIONS TO VSW SOFTWARE

3.1 ERRORS DETECTED AND CORRECTIONS IMPLEMENTED

The following errors were detected as a result of analyzing the VSW software package. Detailed analysis focused on the SWPWDTH and INTEGRAL subroutines (see figure 1-4 in chapter 1) of VSW. Any errors that may exist in subroutines CONINT, GETNAME, FA, and FB remain unidentified. Errors have been corrected as described below, and these corrections are included in the source code listings of subroutines SWPWDTH.MOD and INTEGRAL.MOD.

1. **ERROR**: In subroutine INTEGRAL, the value of $\theta[R(t)]$ was not set to zero for values of slant range R that exceeded the meteorological visibility limit V.

   IMPACT: This error will cause VSW to compute W-values that are too high, especially when V is small relative to the maximum range at which the target can be detected.

   CORRECTION: In subroutine INTEGRAL.MOD, the value of $\theta[R(t)]$ is set to 0 when $R > V$.

2. **ERROR**: The numerical integration algorithm used in subroutine SWPWDTH to compute W erroneously included two extra 0.1-nmi lateral range bins.

   IMPACT: This error will cause VSW to compute W values that are as much as 0.2 nmi too large. The exact value of this error will depend on lateral range curve shape.

   CORRECTION: The numerical integration algorithm in SWPWDTH.MOD sums the correct number of lateral range bins. The probability of detection at the bin midpoint is used in place of the probability at the bin start point.

3. **ERROR:** In subroutine INTEGRAL, the effective target area A was computed incorrectly as

$$A = A_H (h/R) + A_V [1 + (h/R)^2]^{-1/2}.$$

The exponent for the bracketed term should be positive, yielding the expression

$$A = A_H (h/R) + A_V [1 - (h/R)^2]^{1/2}.$$

IMPACT: Several VSW runs were made comparing sweep widths predicted by the erroneous and corrected versions of the program. In the test cases, this computational error did not cause appreciable sweep width error unless the ratio of A_V to A_H was very large (≥ 100).

CORRECTION: The expression for A was corrected in INTEGRAL.MOD. It should be noted that no computer error can occur relative to taking a square root of a negative number in this expression because R is physically constrained to be $\geq h$.

3.2 OTHER SOFTWARE MODIFICATIONS

The following modifications were made to the VSW software package to support the model validation analysis presented in chapter 4. This new software version can be run by substituting the command SEG MODVSW in place of SEG VSW when executing the program. The file MODVSW contains the modified subroutines SWPWDTH.MOD, INTEGRAL.MOD and CONINT.MOD. The main program (VSW) and all other subroutines remain unchanged from their original versions. The only change made to subroutine CONINT was in its calls to the .MOD version of the INTEGRAL subroutine (new variables have been added to the argument list). This change has no effect on the calculations performed by the CONINT subroutine. Thus, CONINT and CONINT.MOD are equivalent. Changes implemented in subroutines SWPWDTH.MOD and INTEGRAL.MOD are documented in the following paragraphs. Note also that the errors identified in section 3.1 were corrected in the .MOD versions of SWPWDTH and INTEGRAL.

1. **Addition of Fixed-Duration Encounters.** The data set analyzed in chapter 4 includes visual distress signalling device (VDSD) targets. Two of these, the hand-held orange smoke (HHOS) and hand-held red flare (HHRF), are pyrotechnic devices that are active only for a fixed amount of time. Modeling searcher encounters with these targets required a modification of the method used in the software to integrate the $\theta[R(t)]$ function. The illustration and definitions of terms given in figure 3-1 are provided to assist the reader in understanding the modifications described below.

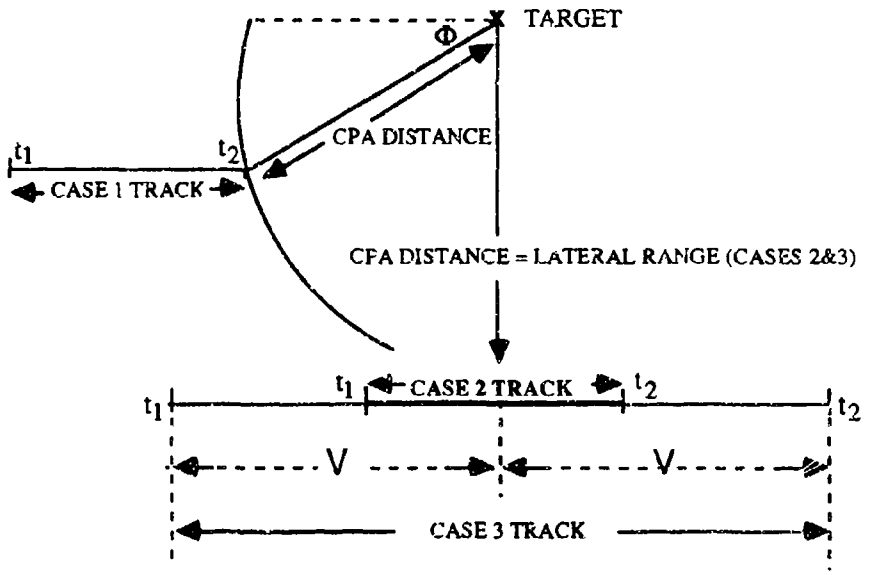

CASE 1: Fixed duration searcher track begins and ends before passing abeam of the target. Searcher position at the end of the encounter (t_2) is offset from the target by angle Φ. Possible values of Φ range from 0 degrees (radial approach to the target) to 90 degrees (track ends directly abeam of the target).

CASE 2: Fixed-duration searcher track passes abeam of the target midway between times t_1 (start of encounter) and t_2. CPA distance complies with the traditional definition of lateral range given in chapter 1.

CASE 3: Similar to CASE 2 except that the searcher-target encounter begins and ends at the limits of meteorological visibility (V). Note that at lateral ranges other than 0 slant range R to the target will exceed the limits of V near the start and end points of the searcher track. (See section 3.1 error number 1.)

Figure 3-1. Illustration of Searcher-Target Encounter Types

CASE 1: In subroutine SWPWDTH.MOD the values of two new variables, PHI and TD, must be input by the user when a CASE 1 encounter is selected. PHI defines the angular offset (in degrees) between the end point of the searcher's fixed-duration track and the target. TD defines the duration of the searcher track in hours. In the case of VDSD targets, TD actually represents the duration of a pyrotechnic device, which in turn defines the effective searcher track duration. The function $\theta[R(t)]$ is integrated only over the path determined by PHI, TD, and searcher speed S in subroutine INTEGRAL.MOD.

CASE 2: In subroutine SWPWDTH.MOD, the only new user input required is the value of TD as defined for CASE 1. The value of PHI is automatically set to 90 degrees and the searcher track is automatically split equally to both sides of the CPA. The function $\theta[R(t)]$ is integrated only over the path determined by TD and S.

CASE 3: This case is equivalent to the searcher track modeled in the unmodified VSW software. No new user input is required for this option. The angle PHI is automatically set to 90 degrees, the searcher track is automatically split evenly to both sides of CPA, and the function $\theta[R(t)]$ is integrated over a path equal to twice the meteorological visibility V in length.

2. **Output of Lateral Range Curve Points and Sweep Width.** In subroutine SWPWDTH.MOD, a file named VSW_OUT is opened for output of lateral range curve and sweep width data. After each run, the user may exit the VSW program and either print the VSW_OUT file or rename it so that it will not be overwritten during the next run of MODVSW.

3. **User Input of C_0 Value.** Subroutine SWPWDTH.MOD allows the user to input a specific value of target intrinsic contrast C_0. In the original version of SWPWDTH, the user specified the target as a PIW or non-PIW, and a default value of 20 or 40 percent, respectively, was assigned to C_0.

CHAPTER 4
COMPARISON OF MODEL PREDICTIONS WITH FIELD EXPERIMENT RESULTS

4.1 VISUAL DISTRESS SIGNAL DETECTION

Reference 2 documents an experiment conducted by the R&D Center in 1986 to determine visual sweep widths for three VDSDs. This test was one in which only parameters that are explicitly considered in the physical detection model were different from the original R&D Center experiments used to determine values of k. Specifically, the values of A_V, A_H, and C_0 are different for the VDSDs. Thus, the VDSD experiment represents model validation method b described in section 2.3.2.

The three VDSDs and their salient characteristics are described in table 4-1. The lateral range curves and sweep widths presented in reference 2 for these devices provide an opportunity to evaluate physical detection model accuracy in accordance with analysis method d described in section 2.3.2.

Table 4-1. VDSD Descriptions

DEVICE DESCRIPTION	USCG NUMBER	MANUFACTURERS	APPLICATIONS	ADVERTISED LUMINOUS INTENSITY (candela)	DURATION
Hand-Held Orange Smoke Flare (HHOS)	160.037	Olin Corp Bristol Corp	Day	N/A	~1 min
Hand-Held Red Flare (HHRF)	160.021	Olin Corp Bristol Corp	Night	500	2 min 3 min
Guest Model 301A Strobe (white)	161.013	Guest Corp	Night	50,000 (peak)	Several days

At this point the reader's attention must be called to a factor that renders application of the physical detection model to night search problems questionable. There is a fundamental difference between the processes by which the human eye detects objects in daylight and dark conditions. Briefly, the shape of the eye's detection lobe is much different at night than during the day. Unlike the narrow lobe depicted for daylight foveal vision in chapter 1, the eye is actually a more effective detector at night in the off-axis or peripheral vision area. This effect reduces the validity of using the function $\theta[R(t)]$ to represent nighttime detection capability. Appendix E of reference 11 contains a good discussion of daylight versus night vision as it applies to visual search problems.

In summary, the 1986 VDSD experiment provides a clear opportunity for model validation with the daytime HHOS detection data. The night detection data involving HHRF and strobe light targets represents a search problem that the physical detection model was not specifically designed to accommodate. The ensuing data analysis should be viewed with this in mind.

4.1.1 Input Parameter Values

Of the search problem parameters that are explicitly considered in the physical detection model, only target areas A_V and A_H and intrinsic contrast C_0 were substantially different in the 1986 experiment as compared to the earlier R&D Center visual detection tests. Equivalent values of meteorological visibility, search altitude, and search speed were available in both data sets. As for parameters that are not explicitly considered in the model; search platform types, environmental conditions, search procedures, and manning were all very similar in both experiments.

Three types of search platform are represented in the 1986 data set: 41-foot utility boats (UTBs), 82- and 95-foot cutters (WPBs), and HH-52A helicopters. All data were collected in good visibility and weather conditions that were compatible with the definition of "fair" provided in reference 1. Time on task for most searches fell within the limits set for "low" in reference 1. The VDSD targets were assumed to be most like a life raft (as opposed to a boat or PIW) because of their strong color contrast with the background (although this was not always true for HHOS). These classifications of searcher type, target type, weather, and time on task determined the values of k to be used in the model. Referring to tables 2 and F-1 in reference 1 and table A 1 in reference 9, we find the following search data file names and k-values are compatible with the 1986 data set:

Searcher Type	Data File Name	k
UTB	GWLF_BOAT_BOATRAFT	.68
WPB	GWLF_CUTR_RAFT	2.75
HH-52A	GWLF_HELO_RAFT	2.57

Of the data file names, "GWLF" refers to good weather, low fatigue; the second group of letters identifies searcher type; and the last group of letters identifies the target type(s) represented. As demonstrated by the "BOATRAFT" target designator in the UTB data file above, search parameter categories were sometimes pooled in reference 1, yielding a single value of k. The k-values shown above were checked by executing option 1 of the VSW software with the same three data file names selected. This procedure yielded k-values of 0.7 for UTBs, 2.63 for WPBs, and 2.57 for HH-52A helicopters. The reason for the slight change in k values for UTB and WPB searchers is not known; the updated values were used in this analysis.

Target areas A_V and A_H were estimated for each of the three VDSDs. In the case of HHOS, A_V and A_H were determined by measuring the smoke plumes produced by each of six HHOS devices and averaging the results. Measurements were taken in light, variable winds of 1 to 4 knots, which were representative of the 1986 experiment. HHRF and strobe areas were estimated based on flame and bulb size, respectively. The values of A_V and A_H used in the model are given below.

VDSD Type	A_V (ft^2)	A_H (ft^2)
HHOS	1026.	2736.
HHRF	0.028	0.0055
STROBE	0.022	0.022

The value of C_0 was the most difficult to estimate for the three VDSDs. In the case of HHOS, the model was run using C_0 values of 20 and 40 percent to bracket the range of daytime values used in reference 1. The smoke from these devices appears bright orange near its source, but pales rapidly as the smoke density decreases with spreading. In the case of night VDSDs, table E-4 in reference 11 provides background brightness values of 10^{-2} foot-Lamberts (ft-L) for full moonlight to 10^{-6} ft-L for full darkness. Various sources place the brightness of the HHRF flame at between 10^5 and 10^7 ft-L. Similar estimates apply to the strobe flash brightness at its peak. Using this range of values, we find that C_0 for the night devices ranges between

$$C_0 = \frac{10^5}{10^{-2}} = 10^7 \times 100 \text{ percent} = 10^9 \text{ percent}$$

and

$$C_0 = \frac{10^7}{10^{-6}} = 10^{13} \times 100 \text{ percent} = 10^{15} \text{ percent.}$$

Obviously these values lie in an altogether different realm of visual contrast than those for daylight viewing of passive targets. Indeed, physical pain is experienced in the dark-adapted eye if these devices are suddenly viewed at close range.

The remaining parameter values that must be specified for the 1986 data set are searcher height h, searcher speed S, and meteorological visibility V. The values of h and S are listed below for each of the three searcher types.

Searcher Type	h (ft)	S (knots)
UTB	10	15
WPB	15	15
HH-52A	1000	85

Table 4-2 provides the average values of V for each searcher type/target type combination represented in the VDSD data set.

Table 4-2. Average Meteorological Visibilities (in nmi) for 1986 Experiment

SEARCHER TYPE	VDSD Target Type		
	HHOS	HHRF	STROBE
UTB	10.5	9.1	9.1
WPB	10.5	9.1	9.1
HH-52A	10.7	9.5	9.5

4.1.2 Sweep Width Comparisons

For each of the 9 searcher/target type combinations, the physical detection model was run to obtain predicted sweep width values for the 1986 experiment. The applicable input parameter values given in section 4.1.1 were used in each model run. The MODVSW version of the physical detection model software, described in chapter 3, was used to compute W for up to 6 cases of interest for each searcher/target type combination. This was done to bracket a range of sweep width values that applied to each searcher/target combination and to provide a sensitivity analysis relative to the choice of C_0 and searcher path.

A variety of searcher paths are represented in the 1986 data sets. Section 3.2 described the 3 types of searcher/target encounters that can be modeled using the MODVSW software. Of the three track cases, cases 1 and 2 represent encounters with pyrotechnic targets such as HHOS and HHRF. Case 3 represents encounters with continuous targets such as the strobe.

Searches for HHOS were modeled at 2 values of offset angle Φ for track case 1. Searcher track case 2 was also modeled for the HHOS target. Two values of C_0 were then selected for each track case yielding the 6 scenarios listed below.

Scenario	Track Case	Target	Angle Φ (track type)	C_0
1	1	HHOS	0 (radial approach)	20
2	1	HHOS	0 (radial approach	40
3	1	HHOS	90 (track ends abeam)	20
4	1	HHOS	90 (track ends abeam)	40
5	2	HHOS	90 (split track)	20
6	2	HHOS	90 (split track)	40

The sweep widths predicted by the physical detection model for these 6 scenarios are shown as a function of searcher type in table 4-3. For $C_0 = 20$ and $C_0 = 40$, sweep width predictions for the three modeled track cases were averaged. This produced upper-and lower-bound W estimates for HHOS with consideration given to the diverse variety of searcher/target encounter paths that occurred during the 1986 experiment. These averaged sweep width predictions are compared in table 4-4 to the corresponding empirical sweep widths from reference 2. The empirical sweep widths and their 80-percent confidence bounds were computed by using a binary, multivariate regression analysis routine to fit a lateral range curve to the appropriate experiment data subset. then integrating to obtain W.

Table 4-3. Sweep Width Predictions (in nmi) for HHOS Targets

Searcher Type	Detection Model Scenario					
	1	2	3	4	5	6
UTB	2.0	3.4	2.2	3.6	3.4	5.3
WPB	4.5	6.7	4.8	7.0	6.2	8.6
HH-52A	3.7	5.9	4.6	7.0	6.1	8.6

Table 4-4. Comparison of Predicted Versus Empirical Sweep Widths (in nmi) for HHOS Targets

Searcher Type	Averaged Detection Model Sweep Width Predictions		Empirical Sweep Width Values (1986 Experiment)	
	Avg. W for $C_0 = 20\%$	Avg. W for $C_0 = 40\%$	W	80% confidence bounds
UTB	2.5	4.1	4.6	3.9 to 5.4
WPR	5.2	7.4	6.9	6.2 to 7.7
HH-52A	4.8	7.2	7.7	6.1 to 9.6

The sweep widths in table 4-4 indicate that the physical detection model estimates agreed well with the empirical data when $C_0 = 40$ percent was input. Model estimates of W for $C_0 = 20$ percent were well below the empirical values. The data in table 4-4 suggest that the k-values determined using life raft targets were suitable for use in extrapolating to new search problems involving HHOS targets. Recall that in this comparison parameters such as searcher type, weather/sea conditions, and marking remained unchanged; only target size was varied. In this restricted case, the model appears to be capable of extrapolating sweep width as long as C_0 can be determined with sufficient accuracy.

For HHRF targets, the same three searcher tracks modeled for the HHOS targets were modeled using a single C_0 value of 10^9. When higher values of C_0 were input, no change in predicted sweep width resulted.

For strobe targets it was necessary to consider only the visibility-limited (case 3) searcher track. Thus, a total of four scenarios were modeled for night VDSDs as listed below. Table 4-5 shows the predicted sweep widths for these four scenarios as a function of searcher type.

Scenario	Track Case	Target	Angle Φ (track type)	C_0
7	1	HHRF	0 (radial approach)	10^9
8	1	HHRF	90 (track ends abeam)	10^9
9	2	HHRF	90 (split track)	10^9
10	3	STROBE	90 (visibility-limited)	10^9

Table 4-5. Sweep Width Values (in nmi) for HHRF and Strobe Targets

Searcher Type	Detection Model Scenario			
	7 (HHRF)	8 (HHRF)	9 (HHRF)	10 (STROBE)
UTB	16.5	16.8	18.0*	18.1*
WPB	18.0*	18.1*	18.2*	18.1*
HH-25A	18.3	18.9*	18.9*	18.9*

* Within 0.2 nmi of maximum possible value for the meteorological visibility specified in table 4-2. This indicates that target detection probability was driven to its maximum possible value in the model at nearly all lateral ranges.

For HHRF targets, sweep width predictions for the three modeled track cases were averaged. As with the HHOS targets, this averaging was done in consideration of the diverse variety of searcher/target encounter paths that occurred during the 1986 experiment. Table 4-6 compares the averaged model predictions of HHRF sweep width to their corresponding empirical values and 80-percent confidence bounds. The data in table 4-6 show that the physical detection model predicts HHRF sweep widths that are 18- to 60-percent higher than those achieved in the field. In all cases, the modeled W value lies outside the 80-percent confidence bounds on the empirical W value. It should be noted that the modeled sweep widths were computed using a lower bound C_0 estimate of 10^9 percent. A C_0 value of 10^{12} percent is probably more representative of the average 1986 experiment conditions, but modeled sweep widths remained unchanged when C_0 values greater than 10^9 were input.

Table 4-6 also compares the modeled sweep width values for strobe signals to the corresponding empirical values from the 1986 experiment. The data in table 4-6 indicate that the physical detection model predicted strobe sweep widths that were more than 4 times greater than those achieved in the field. An obvious question that arises from this result is: Why were the sweep width errors so much larger for strobe targets as compared to those for HHRF targets when

Table 4-6. Comparison of Predicted Versus Empirical Sweep Widths (in nmi) for HHRF and Strobe Light Targets

Searcher Type	Averaged Detection Model Sweep Width Predictions for HHRF	Empirical Sweep Width Values for HHRF (1986 experiment)		Detection Model Sweep Width Predictions for Strobe	Empirical Sweep Width Values for Strobe (1986 experiment)	
		W	80% confidence bounds		W	80% confidence bounds
UTB	17.1	10.7	10.1 to 11.4	18.1	3.9	3.3 to 4.6
WPB	18.1	13.0	12.3 to 13.8	18.1	3.9*	3.3 to 4.6*
HH-52A	18.7	15.4	13.1 to 17.8	18.9	4.4	4.1 to 4.8

*Very limited data set available

C_0 values were identical and target sizes were similar? One likely source of this error is masking of the strobes (which were deployed on anchored life jackets) by ocean waves/swells and simple visual horizon limitations. The physical detection model currently has no mechanism to account for differences between the ocean environment's masking effect on lights deployed less than a foot above the ocean surface and its masking effect on flares held at heights of 8 to 10 feet. The model predicted similar sweep widths for both strobes and flares because model input parameter values were very similar for the two target types. As reflected in the empirical sweep widths, however, there were fundamental physical differences between the two search problems that were not accounted for in the modeling methodology. Note that the model error was smallest for HH-52A helicopter searchers where horizon limits and masking were minimal. Thus, in the case of the strobe targets, a shortfall in the model's applicability to night search problems was magnified by a failure to consider differences in target masking effects.

Overall, the sweep width comparisons made in table 4-6 indicate that the physical detection model in its present form is not capable of accurate extrapolation to night search problems. This result was not unexpected in light of the physical detection model's foundations (see section 4-1, paragraph 3).

4.1.3 Lateral Range Curve Comparisons

As a means of drawing a more detailed comparison between physical detection model outputs and field experiment results, lateral range curves were compared for three searcher/target combinations. The three combinations evaluated were:

1. WPBs searching for HHOS,
2. UTBs searching for HHRF, and
3. HH-52A helicopters searching for strobe lights.

These searcher/target combinations were selected because they are well-represented in the 1986 experiment search data set. The empirical lateral range curves that were fitted to these data sets using regression analysis align extremely well with the sorted raw detection probability data.

In figures 4-1 through 4-3, the raw detection/opportunity proportions, their 90-percent confidence bounds, and regression-fitted lateral range curves for the three data sets are compared to the corresponding lateral range curves predicted by the physical detection model. To facilitate a uniform comparison, a meteorological visibility of 10 nmi was assumed in generating all three sets of plots. The modeled lateral range curves for the three data sets are for a case 1 searcher/target encounter with angle Φ set to 90 degrees in figures 4-1 and 4-2 (HHOS and HHRF targets) and for a case 3 encounter in figure 4-3 (strobe light target).

Inspection of figure 4-1 indicates that, in the case of daylight WPB searches for HHOS, the physical detection model predicted a lateral range curve that was very similar to the empirically-derived curve. The physical detection model appears to predict slightly optimistic detection performance for this searcher/target combination at lateral ranges beyond 2.5 nmi. This tendency resulted in the modeled WPB/HHOS sweep width prediction being slightly higher than the empirically-derived sweep width in table 4-4. Overall, however, the physical detection model performed the extrapolation to the new HHOS target satisfactorily.

Figures 4-2 and 4-3 illustrate that the physical detection model predicted nearly definite detection of both HHRF and strobe light targets over the 0-to 10-nmi lateral range interval. It is obvious from inspection of figures 4-2 and 4-3 that the modeled lateral range curves did not reflect the operational search capabilities of Coast Guard surface and air units searching for night VDSDs. The model appears to be "overdriven" by the high C_0 values that exist for night VDSDs. As discussed in section 4.1, this result is not unexpected when one considers that the foundations of the physical detection model are based on research into daylight, foveal vision.

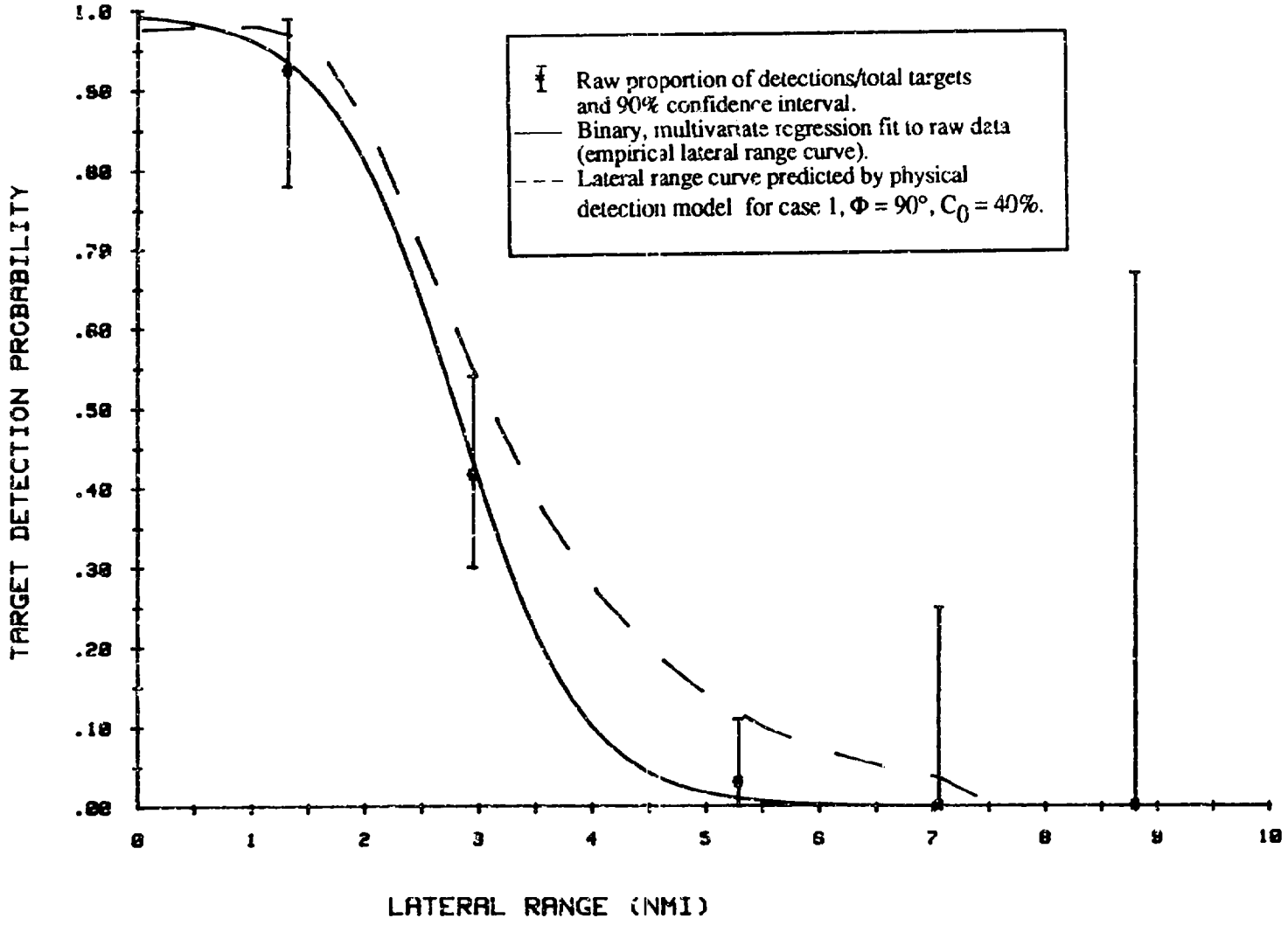

Figure 4-1. Comparison of Empirical and Modeled Lateral Range Curves: WPBs Searching for HHOS Targets

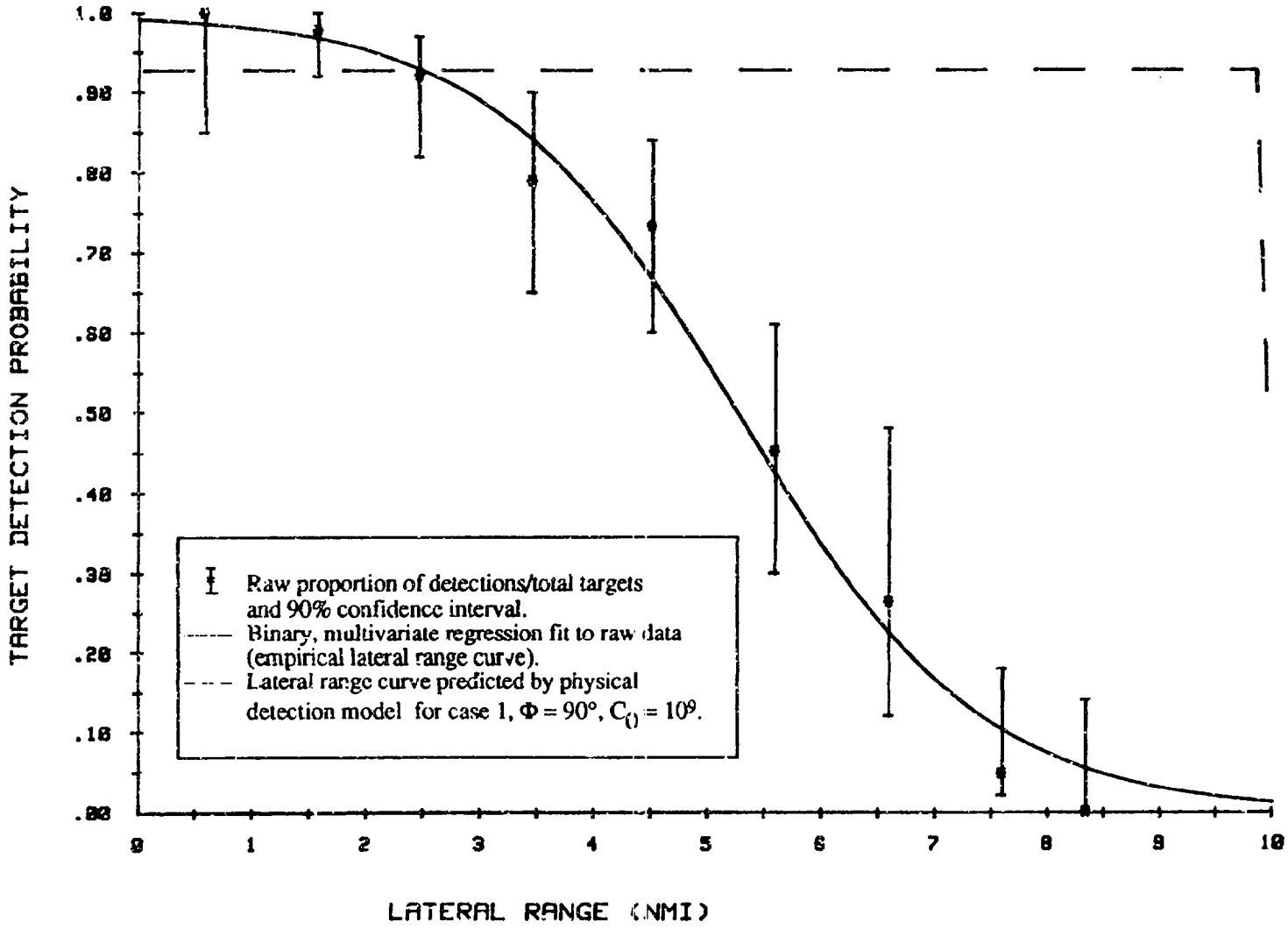

Figure 4-2. Comparison of Empirical and Modeled Lateral Range Curves: UTBs Searching for HHRF Targets

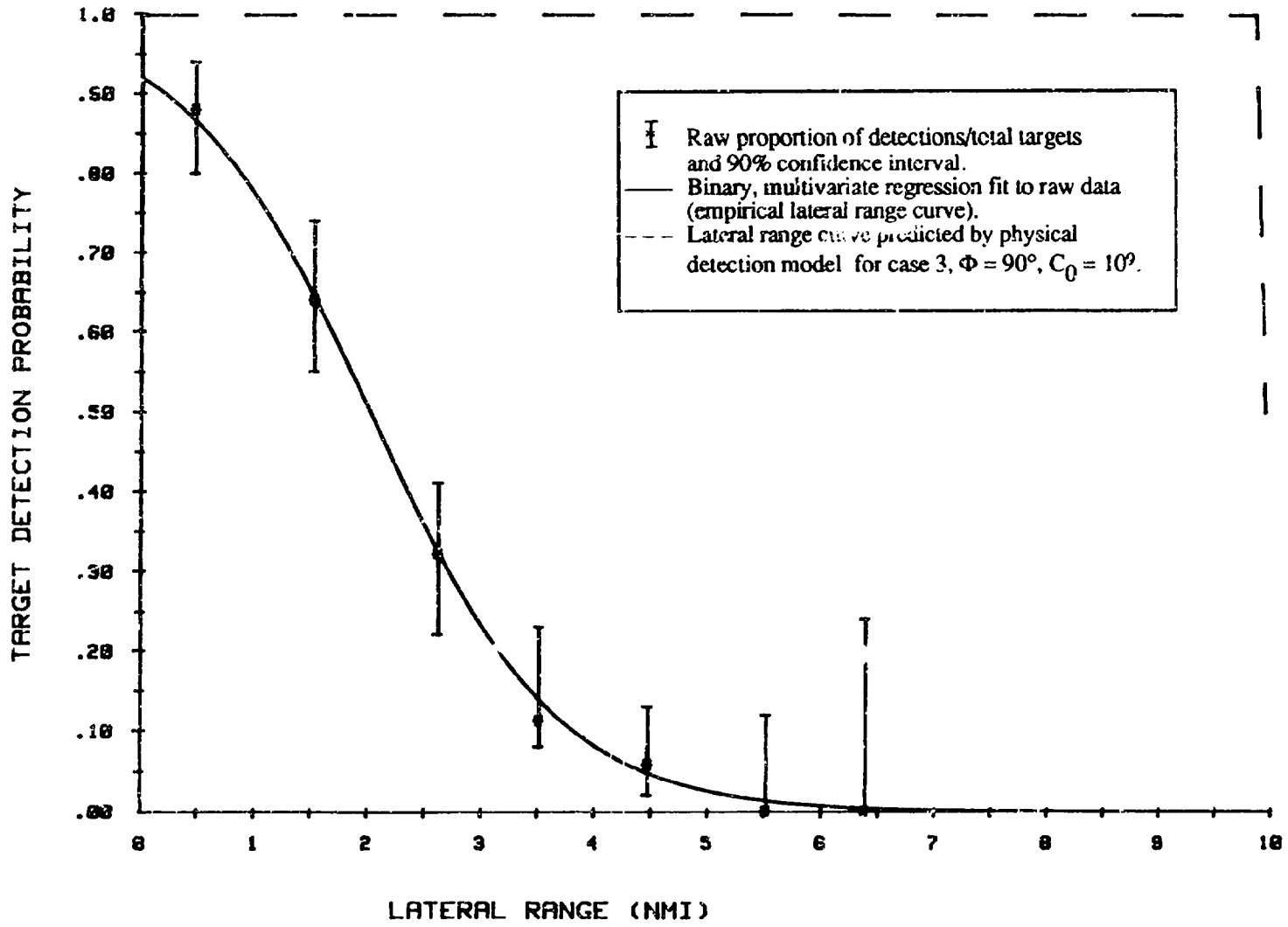

Figure 4-3. Comparison of Empirical and Modeled Lateral Range Curves: HH-52A Helicopters Searching for Strobe Light Targets

4.2 LOW-VISIBILITY DETECTION OF LIFE RAFTS

Reference 3 documents an experiment sponsored by the Canadian Coast Guard in 1986 to determine sweep width for life raft targets in poor visibility conditions. This experiment was a relatively brief precursor to a more extensive experiment that was conducted by Canada in late 1987. Results from the 1987 experiment are not yet available. The 1986 experiment yielded a visual search data set that was adequate for evaluating the physical detection model's ability to extrapolate sweep width to low-visibility conditions for four-person, orange-canopied life rafts.

The Canadian search platform was the 184-foot CCGS JACKMAN. Although considerably larger than a U.S. Coast Guard WPB, this vessel used a similar number of lookouts. Height of eye was estimated to be approximately 25 feet for the Canadian vessel as opposed to approximately 15 feet for the WPB. During the Canadian experiment, a search speed of 9.5 to 10 knots was used; WPB search speeds averaged approximately 14 knots during the USCG visual detection experiments conducted between 1978 and 1981. The life raft targets used by the Canadians were essentially identical to those used by the USCG. Thus, three physical detection model inputs were perturbed in extrapolating sweep width estimates to the Canadian experiment conditions:

1. Meteorological visibility was decreased from an average value of 10.2 nmi to an average of 3.4 nmi,

2. Searcher height was increased from 15 feet to 25 feet, and

3. Searcher speed was decreased from 14 knots to 10 knots.

Of these three perturbations, the meteorological visibility change is by far the most significant.

The physical detection model was run with the following input parameter values to predict a lateral range curve and sweep width for the Canadian experiment:

V = 3.4 nmi
H = 25 feet
S = 10 knots
A_V = 17.2 ft^2
A_H = 31.9 ft^2
C_0 = 40 percent.

A case 3 (visibility-limited) encounter was modeled using a k-value of 1.44. This k-value was determined using option 1 of the VSW software with the search data file "BWAF_CUTR_RAFT" as input. This file represents poor weather (winds > 12 knots and cloud cover > 50 percent), WPB searchers, and four- to six-person orange-canopied life raft targets in the USCG visual detection data base.

Figure 4-4 compares the lateral curve produced by the physical detection model for this search problem to the raw Canadian search data (24 searcher-target encounters at visibilities ≤ 6 nmi) and to the corresponding regression-fitted empirical lateral range curve. Inspection of figure 4-4 reveals that the physical detection model predicted a steeper lateral range curve slope than the empirical data indicate. The modeled lateral range curve overestimated target detection probability at lateral ranges less than 1.2 nmi and drove the probability to zero at approximately 1.75 nmi. The empirical data indicate that a more moderate lateral range curve slope is appropriate. The net effect of these differences in lateral range curve shape was that the physical detection model predicted a slightly higher sweep width than the empirical data indicated. These sweep width values were:

Empirical W: 1.9 nmi
Modeled W: 2.2 nmi (16 percent higher)

This difference between empirical and extrapolated sweep width values is acceptable in light of the considerable uncertainty associated with the small empirical data set. Of concern is the difference in lateral range curve shape. The target detection probability forecast by the model exceeded even the upper 90-percent confidence bound on the empirical data at a lateral range of 0.5 nmi. Concurrently, the model appeared to slightly overstate the dropoff in detection probability as lateral range approached the meteorological visibility limit. For this particular search problem, these two effects counteracted each other sufficiently to yield an acceptable sweep width extrapolation. It appears possible, however, that more significant perturbations of physical detection model input parameters could result in unacceptable sweep width errors caused by inaccurate lateral range curve prediction.

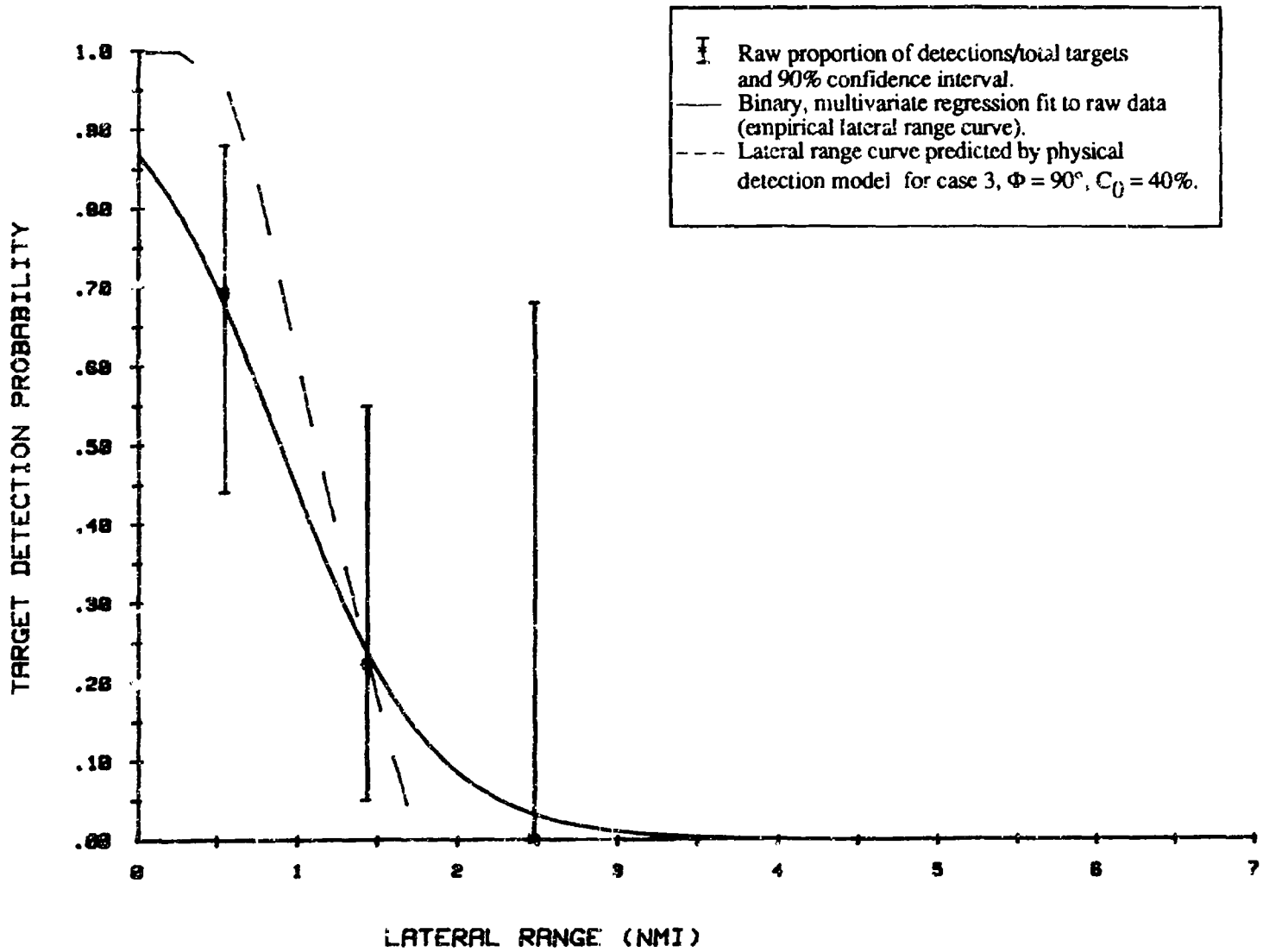

Figure 4-4. Comparison of Empirical and Modeled Lateral Range Curves: Canadian Coast Guard Cutter Searching for Four-Person Life Rafts (Average Visibility = 3.4 nmi)

CHAPTER 5
CONCLUSIONS AND RECOMMENDATIONS

5.1 CONCLUSIONS

1. The Coast Guard's physical detection model appears to be suitable for extrapolating lateral range curves and sweep widths to a limited range of daylight visual search problems that have not been evaluated during field experiments. Visual search problems best suited to the model's extrapolation method are those that involve small perturbations of the critical input parameters search speed, searcher height, target area, and meteorological visibility from values evaluated during field experiments that have been conducted to establish estimates of the model's constant term k.

2. The physical detection model presently lacks the sophistication required to accurately extrapolate lateral range curves and sweep width values to daylight visual search problems that differ substantially from those used to determine values of the input parameter k. In this particular study, for example, the model was shown to predict an inaccurate lateral range curve shape for a new search platform/visibility situation.

3. The physical detection model is not capable of predicting night visual search performance with acceptable accuracy. In this study, the model predicted lateral range curves and sweep widths that were far too optimistic for night visual distress signal targets.

4. Model characteristics requiring improvement fall into two general classifications:

   a. Fundamental model assumptions/foundations that lack validity (such as those described in section 2.3.1, items 1 and 4 and section 2.3.2, items 1 and 3), and

   b. Shortfalls in modeling sophistication (such as those described in section 2.3.1, items 2, 3, and 5 and section 2.3.2, item 2) that require additional analysis and/or research so that the model can accurately fulfill a broader range of Coast Guard sweep width data requirements.

5. The general approach taken in the physical detection model – that of attempting to predict sweep width by analytically representing the visual search/detection process – is a valid one. The complexity of the visual search/detection process, however, demands a great deal of additional research to:

   a. Validate the detection lobe equation's applicability to the operational (non-laboratory) search problem or develop a validated alternative,

   b. Better-define the values of critical model inputs (such as C_0 and k) for a wide range of search problems, and

   c. Describe the behavior of these critical model inputs throughout the searcher-target encounter.

6. The effort required to fully address all of the issues identified above is substantial. This effort could conceivably exceed the effort required to expand Coast Guard sweep width knowledge by conducting visual detection experiments and performing subsequent empirical data analyses. (This is the approach currently used by the R&D Center in the POD/SAR Project.)

5.2 RECOMMENDATIONS

1. Recognizing that the physical visual detection model together with experimentally-determined visual sweep widths forms the basis for the overwater visual sweep width tables used in the National Search and Rescue Manual, a hybrid approach is hereby recommended for near-term expansion and improvement of these sweep width tables. This approach would combine the following elements:

   a. Conduct a series of selected visual detection experiments to develop "anchor values" for sweep width, lateral range curve shape, and detection model parameter k. These experiments should evaluate directly the combinations of searcher type, target type, and environmental conditions that are of greatest relevance to the Coast Guard SAR mission. Criteria for selecting these parameter combinations should be frequency of search problem occurrence, criticality of scenario (i.e., potential for

life and property loss), and potential to support the process described in item b below.

b. Implement selected, low-to-moderate cost/risk improvements, as noted in item 2 below, to the physical visual detection model. Use this improved model to interpolate rather than extrapolate to obtain lateral range curves and sweep widths for search problems that have not been evaluated directly via visual detection experiments in the field.

2. The Coast Guard should take the following actions to effect low-to-moderate cost/risk improvements to the physical detection model:

   a. Adopt the software changes described in chapter 3 of this report as permanent changes to the model's computer implementation.

   b. Incorporate the exact expression for visual angle α given in section 2.3.1 into the model.

   c. Incorporate into the model the effects of earth's curvature, searcher height, and target shape/height on target effective area A.

   d. Apply weighting to the time integration performed in equation 1 to reflect the fact that lookouts concentrate on areas ahead and abeam of the search craft.

   e. Perform field measurements of intrinsic contrast C_0 for common SAR targets at a variety of look angles and cloud cover conditions.

3. The Coast Guard should evaluate the cost/benefit tradeoffs of pursuing the following moderate-to-high cost/risk improvements to the physical detection model:

   a. Conduct field experiments to develop an expression for f(t) in equation 1 that is valid for operational search conditions and scanning searchers who have no prior knowledge of target position.

b. Investigate the effects of color contrast on visual detection and if appropriate, develop a joint color/brightness contrast target characteristic for use in the physical visual detection model.

c. Break out as many search problem parameters as possible from the physical detection model's constant term k and specifically address their influence on the visual detection process within the model. Special emphasis should be given to modeling the effects of sea state, time on task, and search platform characteristics because these parameters have already been shown to exert significant influence on sweep width (see reference 7).

REFERENCES

1. Weisinger, J. R. , Analytical Techniques to Estimate Lateral Range Functions for Visual Detection. D. H. Wagner, Associates, January 1984.

2. Robe, R. Q. and Hover, G. L., Visual Sweep Width Determination for Three Visual Distress Signaling Devices. Report No. CG-D-30-86. U.S. Coast Guard Research and Development Center and Analysis & Technology, Inc., September 1986.

3. Dawe, B. R., Bryant, D. S., and Finlayson, D. J., Search and Rescue Detection Experiment Placentia Bay, NFLD. NORDCO, Ltd. for Transport Canada, September 1986.

4. Koopman, B. O. Search and Screening. OEG Report No. 56, U.S. Navy, 1946.

5. Edwards, N. C.; Osmer, S. R.; Mazour, T. J.; and Bouthilette, D. B. Analysis of Visual Detection Performance (Fall 1978 Experiment). Report No. CG-D-03-79. U.S. Coast Guard Research and Development Center and Analysis & Technology, Inc., December 1978.

6. Edwards N. C.; Osmer, S. R.; Mazour, T. J.; and Hover, G. L., Analysis of Visual Detection Performance for 16-foot Boat and Life Raft Targets. Report No. CG-D-24-80. U.S. Coast Guard Research and Development Center and Analysis & Technology, Inc., February 1980.

7. Edwards, N. C.; Osmer, S. R.; Mazour, T. J.; and Hover, G. L. Factors Affecting Coast Guard SAR Unit Visual Detection Performance. Report No. CG-D-09-82. U.S. Coast Guard Research and Development Center and Analysis & Technology, Inc., August 1981.

8. Letter from Commanding Officer, USCG Research and Development Center to Commander, CG Atlantic Area (Aso), Serial No. 2020/16130/711010.2 with enclosures 1 through 5. 15 July 1981.

9. Weisinger, J. R. and Clark, R. H. User's Guide for VSW (Visual Sweep Width). D. H. Wagner, Associates, February 1984.

10. VSW software source code listings. PRIME computer facility at USCG LANTAREA OCC, Governor's Island, NY.

REFERENCES (cont'd)

11. Koopman, B. O. Search and Screening General Principles with Historical Applications. Pergamon Press (1980).

12. Blackwell, N. J.; Simmons, R. R.; Watson, J. R.; Osmer, S. R.; and Everson, M. L. Preliminary Study on Scanning Techniques Used by U.S. Coast Guard Lookouts During Search and Rescue Missions. Report No. CG-D-50-82 and USAARL 82-7. U.S. Coast Guard Research and Development Center and U.S. Army Aeromedical Research Laboratory. August 1982.

13. Ketchen, H. G.; Nash, L; and Hover, G. L. Analysis of U.S. Coast Guard HU-25A Visual and Radar Detection Performance. Report No. CG-D-29-83. U.S. Coast Guard Research and Development Center and Analysis & Technology, Inc., June 1983.

14. Memorandum from J. R. Weisinger, D. H. Wagner, Associates to LCDR F. Scaraglino, USCG. Subject: Validation of the Visual Detection Methodology, 17 November 1983.